Dynamic Membrane Hyperfiltration," *ASME Paper No. 72-PID-3* (1972).
de Filippi, R. P., and R. L. Goldsmith, "Application and Theory of Membrane Processes for Biological and Other Macromolecular Solutions," in *Membrane Science and Technology*, J. E. Flinn, ed., p. 33, Plenum Press, New York (1970).
Derzansky, L. J., and W. N. Gill, "Mechanisms of Brine-Side Mass Transfer in a Horizontal Reverse Osmosis Tubular Membrane," *AIChE J.*, **20**, 751 (1974).
Goldsmith, R. L., "Membrane Processing in Metal Finishing Industry," *ASME Paper No. 74-ENAS-26* (1974).
———, R. P. de Filippi, S. Hossain, and R. S. Timmins, "Industrial Ultrafiltration," in *Membrane Processes in Industry and Biomedicine*, M. Bier, ed., p. 267, Plenum Press, New York (1970).
Grieves, R. B., D. Bhattacharyya, W. G. Schomp, and J. L. Bewley, "Membrane Ultrafiltration of a Nonionic Surfactant," *AIChE J.*, **19**, 766 (1973).
Koenst, J. W., J. M. Markind, and R. R. Stana, "The Treatment of PWR Nuclear Process Wastes Using Membrane Systems," Proceedings of the 28th Purdue Industrial Waste Conference (1973).
McCutchan, J. W., and V. Goel, "Systems Analysis of a Multi-Stage Tubular Module Reverse Osmosis Plant for Sea Water Desalination," *Desalination*, **14**, 57 (1974).
Michaels, A. S., L. Nelsen, and M. C. Porter, "Ultrafiltration," in *Membrane Processes in Industry and Biomedicine*, M. Bier, ed., p. 197, Plenum Press, New York (1971).
Murkes, J., and H. Bohman, "Mathematical Modelling of Reverse Osmosis and Ultrafiltration Processes," *Desalination*, **11**, 269 (1972).
Nadeau, H. G., and S. Siggia, "Noninstrumental Methods of Analysis," in *Nonionic Surfactants*, M. J. Schick, ed., p. 838, Marcel Dekker, New York (1967).
Okey, R. W., "The Treatment of Industrial Wastes by Pressure-Driven Membrane Processes," in *Industrial Processing with Membranes*, R. E. Lacey and S. Loeb, ed., p. 249, Wiley-Interscience, New York (1972).
Porter, M. C., "Concentration Polarization with Membrane Ultrafiltration," *Ind. Eng. Chem. Product Research Develop.*, **11**, 235 (1972).
———, and L. Nelsen, "Ultrafiltration in the Chemical, Food Processing, Pharmaceutical, and Medical Industries," in *Recent Developments in Separation Science*, N. N. Li, ed., Vol. II, p. 227, Chem. Rubber Co. Press, Cleveland, Ohio (1972).
Rozelle, L. T., J. E. Cadotte, B. R. Nelson, and C. V. Kopp, "Ultrathin Membranes for Treatment of Waste Effluents by Reverse Osmosis," *Appl. Polymer Symp.*, **22**, 223 (1973).
Thomas, D. G., and W. R. Mixon, "Effect of Axial Velocity and Initial Flux on Flux Decline of Cellulose Acetate Membranes in Hyperfiltration of Primary Sewage Effluents," *Ind. Eng. Chem. Process Design Develop.*, **11**, 339 (1972).
Witmer, F. E., "The Use of Semipermeable Membranes to Filter and Renovate Sewage Effluents," Presented at First World Filtration Congress, Paris, France (1974).

Manuscript received March 31, 1975; revision received and accepted June 2, 1975.

Thermal Cracking of Propane and Propane-Propylene Mixtures: Pilot Plant Versus Industrial Data

The product distribution and kinetics of the thermal cracking of propane and propane-propylene mixtures were investigated for a temperature range of 700° to 850°C, exit total pressures from 1.2 to 2 atm. absolute, and steam dilutions of 0.4 and 1.0. The reaction kinetics were determined by two methods. The first uses the equivalent reactor volume concept to reduce the data to isothermicity before attempting the kinetic analysis. The second determines the parameters directly from the nonisothermal data by means of a search routine. Both methods led to a reaction order of 1. The effect of propylene addition was also investigated. Finally, a detailed molecular reaction scheme was derived from a nonisothermal and nonisobaric simulation of the cracking experiments. This scheme was used in the simulation of an industrial cracker and led to excellent agreement, in particular of the product distribution.

P. S. VAN DAMME, S. NARAYANAN, and G. F. FROMENT

Laboratorium voor Petrochemische Techniek
Rijksuniversiteit
Gent, Belgium

SCOPE

The major fraction of the scientific literature on propane cracking deals with radical mechanisms and kinetics of elementary steps, generally studied under conditions which bear little relation to those used in industry. In recent years only a few bench scale studies in flow equipment focused more on directly practical objectives. In spite of this, the design of industrial cracking coils still faces a lack in reliable basic data obtained on a scale large enough to possess the essential characteristics of industrial operation, in equipment sufficiently versatile to permit wide variations in operating conditions and sufficiently instrumented to permit rigorous analysis of the data. The present paper is an attempt to fill this gap.

S. Narayanan is with Kinetics Technology International B.V., The Hague, The Netherlands.

CONCLUSIONS AND SIGNIFICANCE

An extensive experimental investigation on pilot plant scale, covering a wide range of operating variables, has enabled a complex reaction model for propane cracking to be set up. The value of this model is illustrated by its application to the simulation of an industrial propane cracking unit; the propane conversion, the product distribution, the pressure drop, and the temperature profile were in excellent agreement with those observed in the industrial plant.

Hydrocarbon cracking to produce olefines, diolefines, and aromatics is one of the main processes of today's petrochemical industry. Frequently the plant is faced with variations in feedstock compositions, but the product distribution has to match the market demand. The operating conditions then have to be adapted, provided the design permits it. Optimum adaptation is only feasible, without running into operating trouble, when a sufficient knowledge of the fundamentals of the process is available. Too often the design and the variation in operating conditions are based upon an empirical scale-up of pilot plant data which are not always representative.

The present paper reports on a fundamental investigation, covering a wide range of process variables, of the thermal cracking of propane and of mixtures propane-propylene in a pilot cracker. The pilot data are compared with industrial and bench scale results. The data are analyzed to yield the overall kinetics of the process and a molecular reaction scheme permitting the simulation of an industrial cracking unit.

LITERATURE REVIEW

Propane cracking has been studied by quite a number of investigators, but only rather recently in conditions close to industrial operation. Whereas Martin et al. (1959) and Laidler et al. (1962) had observed reaction orders between 1 and 1.5 below 670°C, Buekens and Froment (1968) found that at atmospheric pressure, the order is very close to 1 in the temperature range 700° to 825°C. Yet, the rate coefficients calculated on this basis were found to decrease with conversion, indicating a certain inhibition. To account for this, they introduced an inhibition function ϕ, multiplying the rate coefficient at zero conversion k_o and defined by

$$\phi = \frac{1}{1 + ax} \tag{1}$$

so that

$$k = k_o\phi \tag{2}$$

with

$$k_o = 4.1 \times 10^{11} \exp\left(-\frac{52\,400}{RT}\right) (s^{-1}) \tag{3}$$

$$a = 3.01 \times 10^{-5} \exp\left(\frac{23\,100}{RT}\right) \tag{4}$$

The activation energy of propane cracking considered a first-order reaction would then increase with conversion but decrease as the temperature rises. This might explain values as high as 70 000 kcal/kmole observed by earlier investigators at lower temperatures. Kershenbaum and Martin (1967) found very similar values for the frequency factor of k and for the activation energy in the temperature range 800 to 1000°C.

Illes' (1971) investigation of the overall rate of propane cracking was also limited to atmospheric pressure. He considered the reaction to be first order and accounted for the inhibition by means of a linear law, more restricted in its range of application, of course. Further, the inhibition would increase with temperature.

From a large body of cracking data of single and mixed hydrocarbons, Davis and Farrell (1973) derived first-order kinetic equations. From their general correlation, the following expression for the rate coefficient for propane cracking can be derived:

$$k_{0.1} = 1.68 \times 10^{10} \exp\left(-\frac{46\,500}{RT}\right) \tag{5}$$

where $k_{0.1}$ is the overall first-order rate constant based on an equivalent residence time of 0.1 s.

Herriott et al. (1972) did not limit their kinetic analysis to the overall propane decomposition. They based it upon a reaction scheme comprising eight radical reactions. By adapting the frequency factors and activation energies, they succeeded in fitting satisfactorily their data up to a propane conversion of 70%. In industrial practice, the propane conversion normally exceeds 85%. Also, it should be noted that only wall and not gas temperatures were measured. Herriott et al. also present extensive atmospheric yield data, mainly concerning the primary products. Buekens and Froment presented detailed product distributions at atmospheric pressure, but they did not investigate the influence of total pressure or hydrocarbon dilution.

The cracking of mixtures of propane and propylene was investigated by Robinson and Weger (1971) at a temperature of 1100°C. Propylene was shown to decrease the rate of propane cracking, but no quantitative relation was derived from the data. No systematic pilot plant scale investigation and comparison with industrial data has been reported.

PILOT PLANT DESCRIPTION

The pilot plant unit used for the experimental research is shown in Figure 1. The furnace, built of silica/alumina brick (Li 23), is about 4 m long, 0.7 m wide, and 2.6 m high. It is fired by means of ninety premixed gas burners, mounted with automatic fire checks and arranged on the side walls in such a way as to provide a uniform distribution of heat. The fuel supply system is comprised of a combustion controller that regulates the ratio of fuel to air and the usual safety devices. The furnace is divided into seven separate cells, which can be fired independently to set in any type of temperature profile. Twenty-seven thermocouples are located along the reaction coil, thirteen for measurement of the reacting gas temperature, fourteen for the outside tube wall temperature. In the absence of coke, the temperature difference between the wall and the reacting gas was about 10°C. A few sampling tubes enable the analysis of the reacting gas at intermediate positions. The reaction section of the tube is about 21.75 m long, made of nickel chromium alloy (Alloy 800, Sandvik Sanicro 31), and has an internal diameter of 10 mm. These dimensions were chosen to achieve turbulent flow conditions in the coil with reasonable feed rates. Propane and water enter the furnace at points P and W, respectively. Their flow rates are measured by the rotameters RP and RW. The first cell generates the dilution steam, while the second preheats the incoming propane. Propane is mixed with steam before it enters a mixing chamber

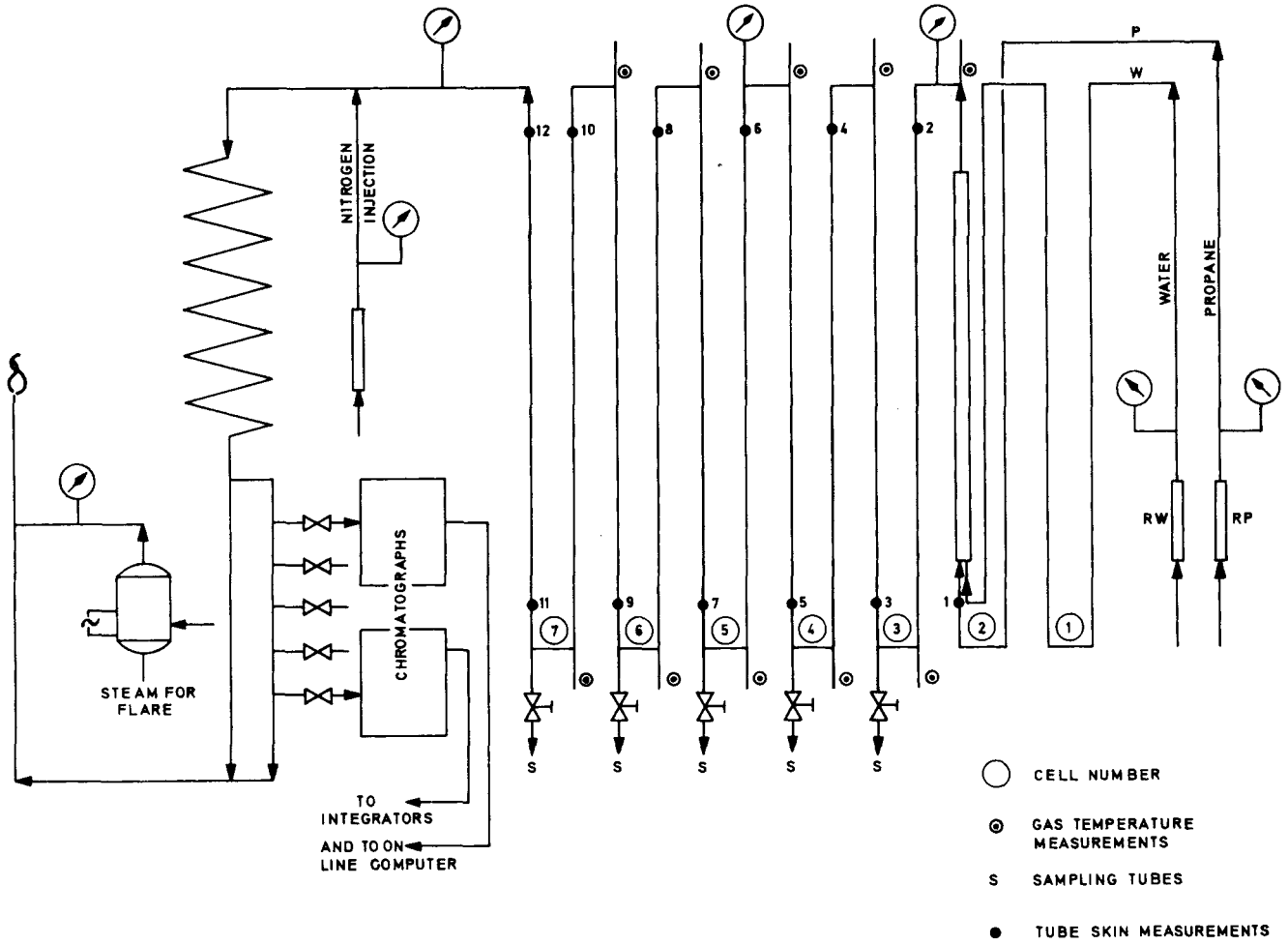

Fig. 1. Pilot plant.

which dampens the pressure fluctuations caused by the water pump. The mixture then flows through the reactor coil. The cracked products leaving the furnace are cooled by a spiral quench cooler. A fraction of the product gas mixture is then withdrawn for on-line analysis, while the rest is sent directly to the flare. Nitrogen injection at the reactor outlet provides an internal standard for the on-line chromatography and contributes to a certain extent to the quenching. The reactor products stream is analyzed by four chromatographs. The first chromatograph (Aerograph 202) determines the nitrogen (internal standard), the C_1, the aromatic fractions; the second (Packard 419) analyzes the C_2, C_3, and C_4 fractions, and the third (PE 11) determines the H_2. Chromatographic details are shown in Table 1. A fourth chromatograph (Varian-FID) was used to determine the aromatics content with greater accuracy. These chromatographs enabled complete analyses of the product streams and complete overall material and carbon balances. The calculations were performed on line by means of PDP-8E process computer with 16K core memory. Runs for which the carbon balances were off by more than 2% were rejected. Carbon disulphide was added to the water to prevent possible wall effects leading to excessive coke formation. The CS_2 concentration in water was 50 p.p.m.

TABLE 1. CHROMATOGRAPHIC ANALYSIS

Chromatograph	Column material	Carrier gas/flow rate 1/hr.	Dimensions, mm	Temp. °C	Products analyzer
1) Aerograph 202	Porapack N 80-100 mesh	H_2/3.6	$L = 1{,}500$, $\phi = 6.3$	30-70	N_2, CH_4
	SE 30 10% chromosorb 80-100 mesh	H_2/3.6	$L = 2{,}000$, $\phi = 3.2$	30-70	C_6H_6, C_7H_8, higher aromatics
2) Packard 419	Durapack 80-100 mesh	H_2/3.6	$L = 2{,}000$, $\phi = 6.3$	30	$N_2 + CH_4$, C_2H_6, C_2H_4 C_3H_8, C_2H_2 i-C_4H_{10}, C_3H_6 1-C_4H_8, 2-C_4H_8 1, 3 C_4H_6
3) PE 11	Porapack Q 80-100 mesh	N_2/2.5	$L = 3{,}000$, $\phi = 3.2$	50	H_2, CH_4
4) Varian 1200 FID	SE 30, 10% 80-100 mesh	N_2/1.5	$L = 3{,}600$, $\phi = 3.2$	20-130 20°/min	C_4, C_5, benz, tol, xyl.

Table 2. Classification of Experiments

Class	Total outlet pressure (atm. abs.)	Steam dilution (kg of steam/kg of propane)	Inlet propane partial pressure (atm.)
1	1.4	0.4	0.75
2	1.4	1.0	0.45
3	2.0	0.4	1.1
4	2.0	1.0	0.65

EXPERIMENTAL PROGRAM

The propane used for the thermal cracking had the following composition:

C_2H_6	from	0.2 to	2.5%	by weight
C_3H_8	from	99.0 to	96.0%	by weight
C_3H_6	from	0.2 to	0.6%	by weight
iC_4H_{10}	from	0.5 to	0.9%	by weight

The following range of process variables was investigated in the present work.

Variable	Range
Propane flow rate, kg/hr.	2-5
Steam to propane ratio, kg/kg	0.2-1.0
Outlet temperature, °C	700-870
Outlet pressure, atm. abs.	1.2-2.3
Reynolds number	5 000-10 000
Pressure drop, kg/cm²	0.3-0.5

The temperature profile and the residence time were varied considerably, owing to the flexibility of the furnace. For instance, runs at very low space times were conducted with only the last two reaction cells kept at high temperature, instead of five. The study of propane cracking was based on about 360 experiments, which were classified as shown in Table 2.

These experimental results served as a basis for the study of the product distribution, the kinetics of overall rate of propane disappearance, and a molecular reaction scheme for the cracking. In addition, forty-five experiments were performed with mixtures of propane and propylene containing 0.5, 3, and 5 wt. % propylene.

PRODUCT DISTRIBUTIONS

Propane Cracking

The major products of cracking are methane, ethylene, hydrogen and propylene. The product distribution mainly depends on the conversion level but also on both the partial pressure of propane and the total pressure. The influence of these variables was investigated by means of four classes of experiments, already shown in Table 2. The results expressed in terms of weight yields (kilogram of a product/100 kg propane fed), as is customary in industrial practice, are shown in Figures 2 to 9. Further, the influence of the partial and total pressure is shown in Table 3.

The ethane yield is also strongly pressure dependent, but this dependence could not be determined accurately in this work since the feed contained varying amounts of ethane.

A typical product distribution obtained in the pilot plant is shown in Table 4, along with industrial data. The agreement is remarkable.

Cracking of Mixtures Propane Propylene

Experiments were performed with propane feed containing 0.5, 3, and 5 wt. % of propylene. Such feeds are normally encountered in industrial plants. Propane conversion

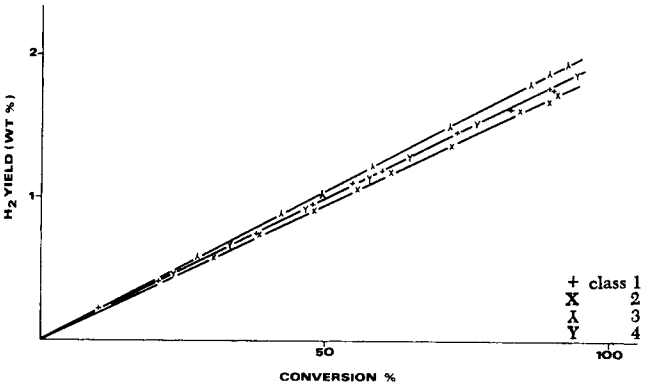

Fig. 2. Hydrogen yields as a function of propane conversion.

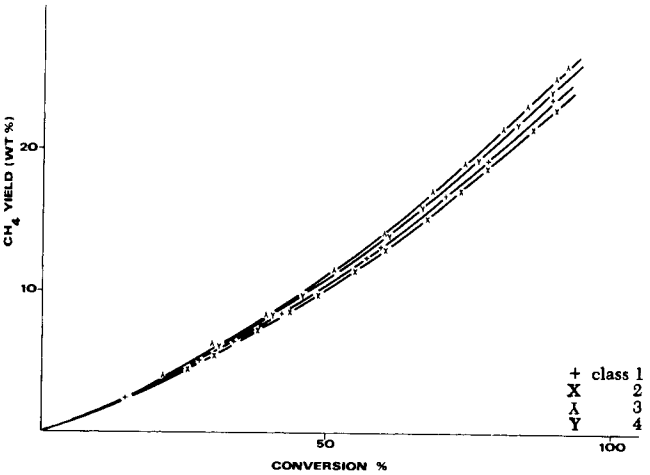

Fig. 3. Methane yields.

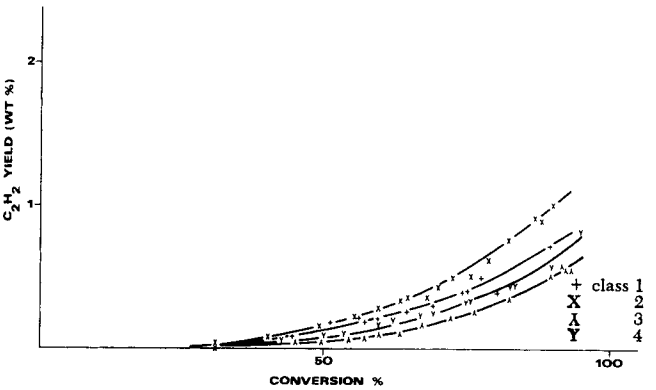

Fig. 4. Acetylene yields.

Table 3. Influence of Propane Partial Pressure and of Total Pressure on the Yields

Components	Increase of Partial pressure	Increase of Total pressure
H_2	+	+
CH_4	+	+
C_2H_2	−	−
C_2H_4	−	−
C_3H_6	0	+
C_4H_6	+	−
C_4H_8	−	−
C_5^+	+	+

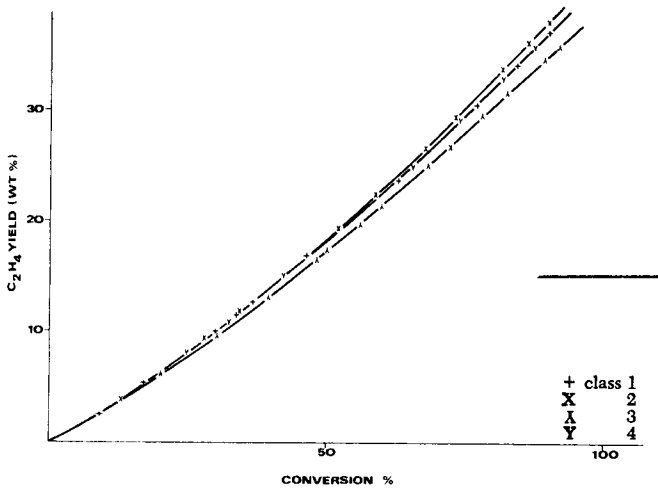

Fig. 5. Ethylene yields.

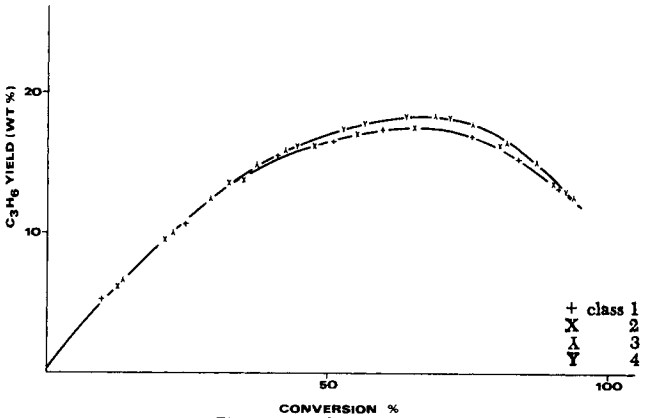

Fig. 6. Propylene yields.

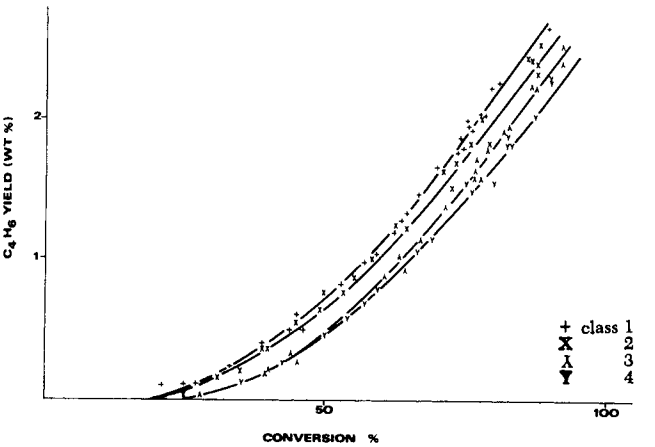

Fig. 7. 1-3 butadiene yields.

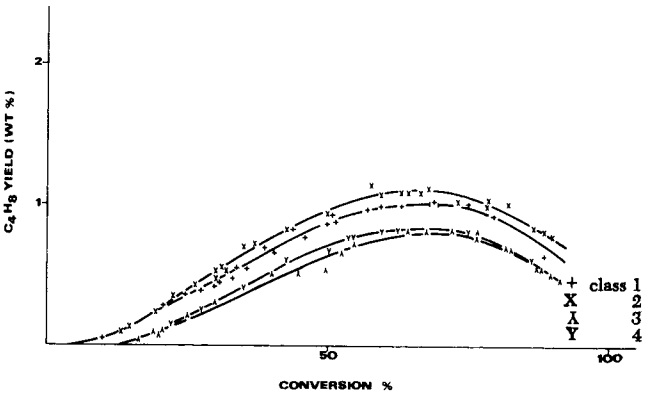

Fig. 8. 1-butene yields.

TABLE 4. COMPARISON OF PILOT PLANT AND INDUSTRIAL DATA

	Pilot plant	Industrial
Propane conversion, %	89.6	90.6
H_2 weight yields, %	1.8	1.2
CH_4	24.9	24.0
C_2H_2	0.5	0.4
C_2H_4	35.0	34.5
C_2H_6	3.5	5.8
C_3H_4	0	0.5
C_3H_6	14.7	14.7
C_3H_8	10.4	9.3
C_4H_6	2.3	1.5
C_4H_8	0.6	1.0
C_4H_{10}	0	0.1
C_5^+	6.3	7.0
Propylene/ethylene	0.42	0.43
P_{out}, atm. abs.	2.0	2.0
Reference temperature, °C	835	838
Steam dilution, kg/kg	0.4	0.4

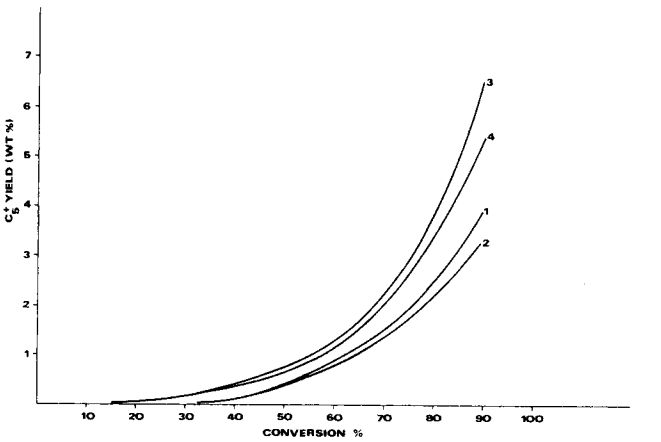

Fig. 9. C_5+ yields.

is lowered by the addition of propylene more than by the effect of the lower partial pressure. Table 5 compares the product distribution obtained, for identical reaction conditions, with pure propane and with a feed containing 5 wt. % of propylene, and at a propane conversion of 83.3%. The addition of propylene markedly decreases the ethylene and butadiene yield without influencing the propylene yield, while C_5+ is significantly increased.

Clearly, reactions between ethylene, propylene, and butadiene are responsible for this. Also shown is a product distribution calculated on the basis of those obtained with pure propane and pure propylene, assuming no interaction and based on the product distribution for propylene cracking obtained by Kunugi et al. (1970). The experimental yields for methane and ethylene are higher than those calculated, while the experimental propylene yield is lower. Propylene is probably interacting with hydrogen radicals to form *i*-propyl radicals. The *i*-propyl radicals isomerize into *n*-propyl radicals, and these decompose into ethylene and methane, increasing the respective yields with respect to the noninteractive values.

Table 5. Comparison of Product Distributions, in Weight Percent, Obtained from Pure Propane and Mixtures of Propane Propylene

	Pure propane		Mixture		
	Feed	Products	Feed	Experimental Products	Calculated Products
H_2		1.6		1.6	1.6
CH_4		20.8		21.3	20.5
C_2H_2		0.5		0.4	0.5
C_2H_4		33.7		31.5	30.8
C_2H_6	1.26	2.8	0.19	2.4	2.3
C_3H_6	0.52	16.8	5.32	16.7	17.8
C_3H_8	97.08	15.7	93.45	15.7	15.7
C_4H_6		2.4		1.9	2.3
C_4H_8		0.8		0.7	0.7
iC_4H_{10}	1.14		1.14		
nC_4H_{10}		0.2		0.2	0.2
C_5^+		4.7		7.5	7.5

Propane conversion % : 83.3
Exit total pressure, atm. abs. : 1.4
Inlet propane partial pressure, atm.: 0.74
T_R, °C : 825

KINETIC ANALYSIS

The analysis of thermal cracking data is rendered difficult because of the inevitable temperature profile prevailing in the reactor. Even if large portions of the tube are at a uniform temperature, as is possible in bench scale equipment, parts of the preheat and quench sections are at temperature levels where reaction cannot be excluded. Froment et al. (1961) applied the equivalent reactor volume concept to correct for nonisothermality, mainly in the preheat and quench sections. The pilot plant data reported here are a much more severe test for its application, however, on account of the steadily rising temperature profile. With such a profile, which is also encountered in industrial practice, an important fraction of the tube is at temperatures far away from the selected reference temperature. In addition, the experiments were not isobaric.

A different approach, which is much more demanding from the computational standpoint, however, involves an integration of the continuity equation for propane along the experimental temperature and pressure profile, with successive improvement of the kinetic parameters until a satisfactory fit of experimental and calculated profiles is arrived at. Both ways of approach will be discussed in detail and their results compared.

Pseudo-Isothermal Analysis

The kinetic study along the pseudo isothermal approach requires data of propane conversion vs. space time V_E/F_o as illustrated by Figure 10 for the data of class 3. To eliminate the influence of the temperature profile, the space time is based on the equivalent reactor volume V_E. The equivalent reactor volume V_E is defined as that volume which, at a reference temperature T_R and at a reference total pressure P_R, would give the same conversion as the actual reactor volume, with its temperature and pressure profiles.

By starting from a differential volume element

$$r_{T_R,P_R}dV_E = r_{T,P}dV \tag{6}$$

the following expression is obtained for a reaction with order n:

$$V_E = \int_0^v \left(\frac{PT_R}{P_RT}\right)^n \exp\left[\frac{E}{R}\left(\frac{1}{T_R} - \frac{1}{T}\right)\right] dV \tag{7}$$

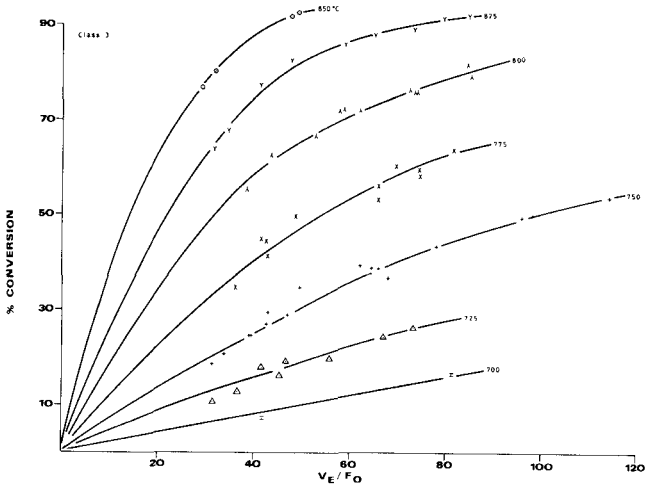

Fig. 10. Propane conversions vs. ratio V_E/F_0.

The calculation of V_E, therefore, requires a priori knowledge of the activation energy, which is precisely one of the parameters to be determined by the kinetic analysis. Froment et al. (1961) have worked out a method for determining a first estimate of the activation energy. In the present case, sufficiently reliable data were available in the literature. A value of 55 000 kcal/kmole was used. This was close enough to the final value determined by the kinetic analysis to render any iteration superfluous. The reference temperature was taken as the arithmetic mean of the temperatures in the last 40% of the tube length. The reference pressure was the atmospheric pressure. The concept reduced in some cases the actual volume by a factor 3, particularly with the experiments conducted with only the last two reaction cells kept at high temperatures, instead of five. In the diagram of conversion vs. V_E/F_o, such as Figure 10, the experimental points for the propane conversion obtained with only two cells are completely in line with those representing the runs with the five reaction cells at high temperature. This strongly supports the use of the equivalent reactor volume concept as a tool for kinetic analysis.

Having thus reduced the data to sets of pseudo isothermal data at a number of reference temperatures, the kinetic analysis may be tackled along classical lines. What is meant here by kinetic analysis is the determination of an overall rate equation for propane disappearance of the power law type, that is, not accounting explicitly for the radical nature of the reaction. The continuity equation for propane may be written

$$F_o dx = kC^n dV_E \tag{8}$$

or, more explicitly

$$F_o dx = k\left[\frac{1-x}{1+\delta+(\epsilon-1)x}\right]^n \left(\frac{P_R}{RT_R}\right)^n dV_E \tag{9}$$

where

δ = dilution ratio, ϵ = expansion, $k = A\exp(-E/RT_R)$

Integration of (9) for $\epsilon = 2$ leads to

$$k\frac{V_E}{F_o}\left(\frac{P_R}{RT_R}\right)^n = \int_o^x \left(\frac{1+\delta+x}{1-x}\right)^n dx \tag{11}$$

The right-hand side of this equation was integrated analytically for $n = 0.5$, 1.0, 1.5, and 2.0. Then, for experiments at equal conversion but different propane partial pressures, the rate coefficient was plotted vs. the order, as illustrated by Froment et al. (1961). The intersection of the curves

Table 6. Reaction Order at Various Levels of Conversion and Temperature

Conversion x, %	Temperature T_R, °C	Order n
25	740	0.98
77	815	0.99
82	820	1.02

Table 7. Kinetic Parameters for the Four Classes of Experiments Obtained by Pseudo Isothermal and Nonisothermal Analysis

	Pseudo isothermal first order		Nonisothermal order, n left open		
	E	A	n	E	A
Class 1	51,000	$1.08 \cdot 10^{11}$	1.005	51,167	$1.17 \cdot 10^{11}$
Class 2	51,000	$1.17 \cdot 10^{11}$	1.02	50,682	$1.01 \cdot 10^{11}$
Class 3	49,300	$4.5 \cdot 10^{10}$	1.04	51,112	$1.16 \cdot 10^{11}$
Class 4	50,200	$6.97 \cdot 10^{10}$	0.996	49,568	$5.42 \cdot 10^{10}$

related to the different experiments corresponds to the order of the reaction. Table 6 shows that the order is close to 1 over the entire range of temperatures and conversions investigated in this work.

If, then, the order is 1, the corresponding rate coefficients may be calculated and the activation energy derived from the Arrhenius plot of Figure 11 by means of linear regression. This was done separately for each of the four classes of experiments mentioned above. The results are reported in Table 7 from which it is clear that the kinetic parameters are unaffected by the partial or the total pressure, a conclusion which supports the validity of the proposed first-order kinetic equation.

Nonisothermal Analysis

In the nonisothermal approach, k in (8) is defined as $A \exp(-E/RT)$. The continuity Equation (9) is then numerically integrated along the tube length for each experiment, accounting for the gas temperature and pressure profile, with estimated values for A, E, and n. The experimental and the calculated propane exit conversion are compared with one another to guide the choice of improved estimates of the parameters. The integration was performed by means of a Runge-Kutta-Merson routine. A sum of squares of deviations $\Sigma(x - x)^2$ was used as objective function, to be minimized by the appropriate choice of A, E, and n. The optimization method used in the improvement of the parameters was a Marquardt routine. The strong correlation between A and E necessitated a reparameterization over

$$A' = A \exp\left(-\frac{E}{RT_m}\right) \tag{12}$$

where T_m is the average of all the temperatures, so that Equation (9) becomes

$$F_o dx = A' \exp\left(\frac{E}{RT_m} - \frac{E}{RT}\right) \left[\frac{1-x}{1+\delta+(\epsilon-1)x}\right]^n \left(\frac{P}{RT}\right)^n dV_E \tag{13}$$

This procedure was applied to the data of the four classes of experiments, and the results are also shown in Table 7. Again, no trend is visible with respect to total or partial pressure, and the values of the order, the frequency factors, and activation energies are in excellent agreement with those obtained by means of the pseudo isothermal analysis

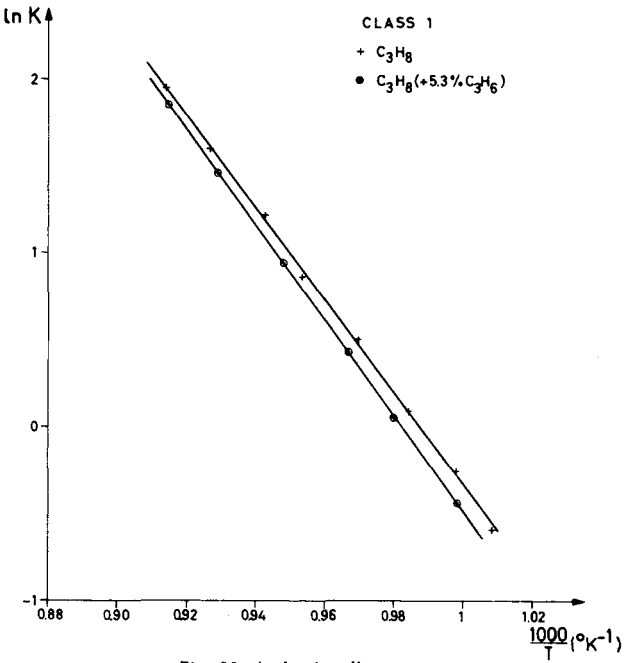

Fig. 11. Arrhenius diagram.

based upon the equivalent reactor volume concept. This strongly supports the application of this concept, even for such severe conditions as those of the present work, provided the temperature profile of the reacting gas is accurately known, and reasonably accurate estimates of the activation energy are available. The nonisothermal analysis was also applied to a selected number of representative experiments of the four classes together. The results were $n = 1.002 \pm 0.02$, $E = 50\,834 \pm 1\,800$, $A = 1.06 \times 10^{11}$. The above results are in excellent agreement with those of Buekens and Froment (1968) and Herriott et al. (1972).

Influence of Propylene Addition on the Rate of Propane Cracking

The inhibitory effect of propylene addition on the rate of propane cracking is illustrated for a few reaction conditions in Figure 12, in which the rate coefficient for the disappearance of propane is plotted vs. the propylene content.

MOLECULAR REACTION SCHEME FOR PROPANE CRACKING

So far, the kinetic analysis was limited to the overall propane disappearance. In attempting to describe the detailed kinetics and product distributions of a thermal cracking reaction, two ways of approach are possible. The first is based upon a radical scheme for the reactions. Serious problems arise in integrating the differential equations because of their stiff character. To avoid the difficulties, the pseudo steady state approach has been used by several authors (Lichtenstein, 1964; and Shah, 1967). The second approach consists of approximating the true nature of the reactions by a so-called *molecular scheme*. The model used here is of the second type and was developed on the basis of a large number of simulations of the pilot plant runs. Models reported so far were considerable, extended to include secondary reactions and to permit the predictions of yields associated with propane conversions as high as 90%. The final scheme, with the corresponding frequency factors and activation energies, arrived at by trial and error, is given in Table 8. Reactions 1 and 2 are the main reactions.

Table 8. Molecular Reaction Scheme for the Simulation of Gas Cracking

Reactions	A (s^{-1}) or + ($kmole^{-1}\ m^3\ s^{-1}$)	E (kcal/mole)
1. $C_3H_8 \rightarrow C_2H_4 + CH_4$	1.6×10^9	44,000
2. $C_3H_8 \rightarrow C_3H_6 + H_2$	2.0×10^9	44,000
3. $2C_3H_8 \rightarrow C_2H_6 + C_4H_{10}$	2.2×10^9	54,000
4. $2C_3H_8 \rightarrow C_3H_6 + C_2H_6 + CH_4$	1.1×10^9	48,000
5. $C_2H_6 \rightarrow C_2H_4 + H_2$	0.34×10^{13}	60,000
6. $2C_2H_6 \rightarrow C_2H_4 + 2CH_4$	3.9×10^{12}	67,000
7. $2C_2H_6 \rightarrow C_3H_8 + CH_4$	0.5×10^{11}	50,000
8. $2C_3H_6 \rightarrow 3C_2H_4$	1.3×10^{10}	50,000
9. $C_3H_6 + H_2 \rightarrow C_2H_4 + CH_4$	1.0×10^{15}	60,000
10. $C_3H_6 \rightarrow C_2H_2 + CH_4$	1.4×10^{10}	50,000
11. $C_2H_4 + H_2 \rightarrow C_2H_6$	0.68×10^{13}	52,000
12. $C_2H_4 \rightarrow C_2H_2 + H_2$	6.0×10^{13}	76,000
13. $3C_2H_4 \rightarrow 2C_3H_6$	1.3×10^{11}	45,000
14. $2C_2H_2 + H_2 \rightarrow C_4H_6$	$+6.0 \times 10^{13}$	45,000
15. $C_2H_2 + 2H_2O \rightarrow 2CO + 3H_2$	3.5×10^{11}	62,000
16. $C_2H_2 + C_3H_6 \rightarrow C_5H_8$	$+9.0 \times 10^{16}$	64,000

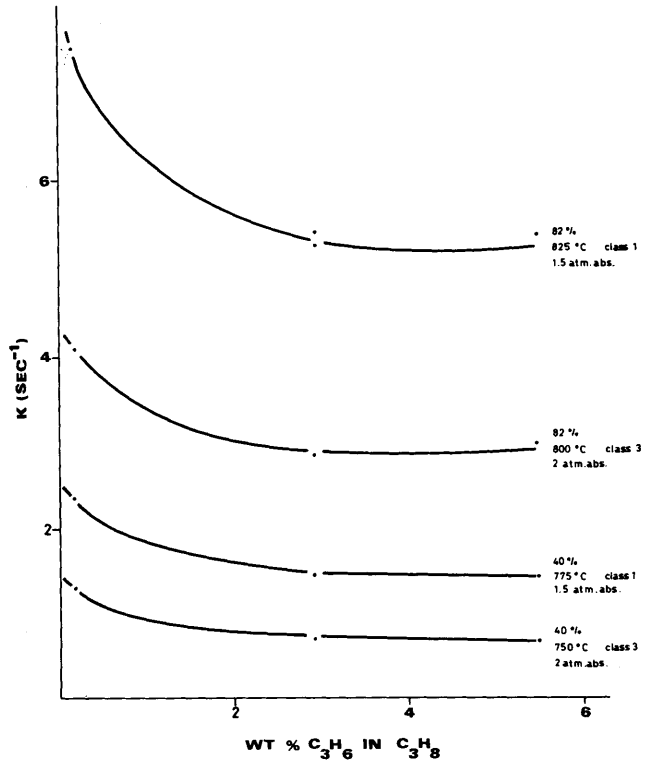

Fig. 12. Influence of propylene on the rate coefficient for propane cracking.

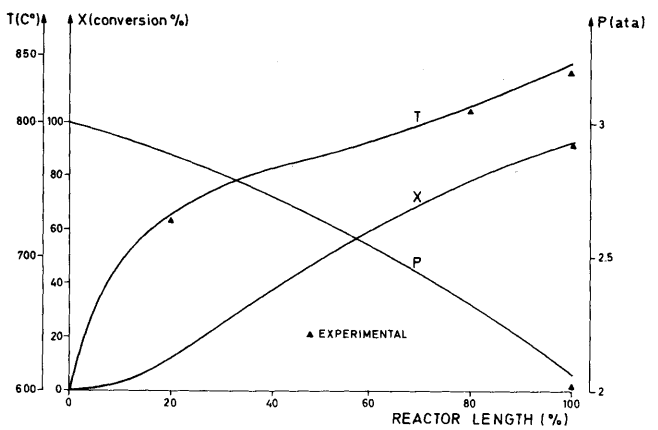

Fig. 13. Plant simulation. Conversion, temperature, and total pressure profiles along the coil. Curves: model simulation. Points: plant data.

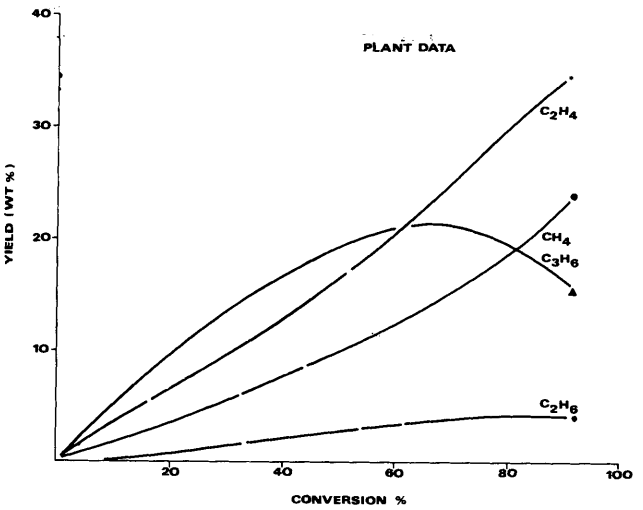

Fig. 14. Plant simulation. Simulated products distribution profiles. Points: plant data.

INDUSTRIAL REACTOR SIMULATION

The simulation of an industrial unit for the thermal cracking of propane requires the following set of continuity equations for the components, the energy equation, and the pressure drop equation to be integrated:

$$\frac{dF_j}{dz} = -R_j\,\Omega = -\left(\sum_i s_{ij}\,r_i\right)\Omega \qquad \begin{matrix} j = 1 \ldots\ldots 10 \\ i = 1 \ldots\ldots 16 \end{matrix} \tag{14}$$

$$\frac{dT}{dz} = \frac{1}{\sum_j F_j\,c_{pj}}\left[Q(z)\,\pi d_t + \Omega \sum_i r_i\,(-\Delta H)_i\right] \tag{15}$$

$$-\frac{dP}{dz} = \alpha\left(\frac{2f}{d_t} + \frac{\xi}{\pi r_b}\right)\frac{RT}{M_m P g}\,G^2 \tag{16}$$

where j represents the components, i the number of reactions, s_{ij} the stoichiometric coefficients, R_j the total rate of change of the component j, and r_i the rate of reaction i. $Q(z)$ is the heat flux, which varies along the coil, ξ a friction factor for the pressure drop in the bends, and conversion factor from kgf/m^2 to atm. The industrial reactor had a coil length in the radiant section of the furnace of 95 m. The length of the straight portions of the coil was 8.85 m, the length of the bends 0.554 m. The radius of the latter was 0.178 m. The internal diameter of the tube was 0.108 m. The total feed per coil was 86.35 $kg/m^2\ s$, and the steam dilution amounted to 0.4 kg/kg propane. The

inlet pressure was 3 atm.abs. and the outlet pressure 2 atm.abs. The following temperature measurements were available: inlet, 600°C; 20% of coil length, 740°C; 80% of coil length, 812°C; outlet, 838°C. The following heat flux profile was generated from independent simulations of the heat transfer in the fire box: first tube, 22 kcal/m² s; second tube, 20; third, 18; fourth, 17; fifth, 15; sixth, 13; seventh, 11; eight, 8; ninth and tenth tube, 6. With this heat flux profile, the conversion, temperature, and total pressure profiles of Figure 13 were obtained. The agreement with the industrial data is really excellent. The use of the molecular reaction scheme of Table 8 also enabled the product distribution at the exit of the coil to be compared with the industrial data. This is done in Figure 14, which also shows an excellent agreement.

ACKNOWLEDGMENT

The authors are grateful to the "Fonds voor Kollektief Fundamenteel Onderzoek" for support of Research Project nr. 919.

NOTATION

a = inhibition constant
A = frequency factor, s^{-1}
C = concentration, kmole/m³
c_p = specific heat of gases, kcal/kmole °C
d_t = internal tube diameter, m
E = activation energy, kcal/kmole
F_o = molar flow rate of propane at inlet, mole/s
F_j = molar flow rate of component j, kmole/s
G = mass flow velocity, kg/m² s
ΔH = heat of reaction, kcal/kmole
k = rate coefficient, s^{-1} or $\text{kmole}^{-(n-1)}\text{m}^{3n-3}\text{s}^{-1}$
k_o = rate coefficient at zero conversion, s^{-1} or $\text{kmole}^{-(n-1)}\text{m}^{3n-3}\text{s}^{-1}$
n = order of reaction
P = total pressure, atm. abs.
P_R = reference totai pressure, atm. abs.
$Q(z)$ = heat flux, kcal/m² s
R = gas constant, 1.987 kcal/kmole °C or 0.082 $\frac{\text{m}^3 \text{ atm.}}{\text{kmole °K}}$ in (16)
r = rate of reaction, kmole/m³s
r_b = radius of bend of the coil, m
S_{ij} = stoichiometric coefficients of component j in equation i
T = temperature, °K or °C
T_R = reference temperature, °K
V_E = equivalent reactor volume, m³
x = conversion
Z = distance along the coil, m

δ = dilution ratio, kmole steam/kmole propane at inlet
ϵ = expansion factor, kmole products/kmole propane cracked
ϕ = inhibition function
Ω = cross sectional area of coil, m²

Subscripts

i = i^{th} stoichiometric equation
j = component

LITERATURE CITED

Buekens, A. G., and G. F. Froment, "Thermal Cracking of Propane," *Ind. Eng. Chem. Process Design and Develop.*, **7**, 435 (1968).

Davis, H. G., and T. J. Farrel, "Relative and Absolute Rates of Decomposition of Light Paraffins under Practical Operating Conditions," *ibid.*, **12**, 171 (1973).

Froment, G. F., H. Pijcke, and G. Goethals, "Thermal Cracking of Acetone—I & II," *Chem. Eng. Sci.*, **13**, 173 (1961); **13**, 180 (1961).

Herriott, G. E., K. E. Eckert, and L. F. Albright, "Kinetics of Propane Pyrolysis," *AIChE J.*, **18**, 84 (1972).

Illes, V., "The Pyrolysis of Gaseous Hydrocarbons III," *Acta. Chim. Acad. Sci. Hung.*, **67**, 41 (1971).

Kershenbaum, L. S., and J. J. Martin, "Kinetics of the Non-isothermal Pyrolysis of Propane," *AIChE J.*, **13**, 148 (1967).

Kunugi, T., K. Soma, and T. Sakai, "Thermal Cracking of Propylene," *Ind. Eng. Chem. Fundamentals*, **9**, 319 (1970).

Laidler, K. J., N. H. Sagert, and B. W. Wojciechowski, "Kinetics and Mechanisms of the Thermal Decomposition of Propane," *Proc. Roy. Soc.*, **A270**, 242 (1962).

Lichtenstein, L., "Design Cracking Furnaces by Computer," *Chem. Eng. Progr.*, **60**, No. 12, 64 (1964).

Martin, R., M. Dzierzynski, and M. Niclause, "La Décomposition Thermique du Propane," *J. Chim. Phys.*, **61**, 286 (1964).

Robinson, K. K., and E. Weger, "High Temperature Pyrolysis of Propylene-Propane Mixtures," *Ind. Eng. Chem. Fundamentals*, **10**, 198 (1971).

Shah, M. J., "Computer Control of Ethylene Production," *Ind. Eng. Chem.*, **59**, 70 (1967).

Manuscript received March 7, 1975; revision received June 24, and accepted June 25, 1975.

A Thermodynamic Method of Predicting the Transport of Steroids in Polymer Matrices

Application of Hildebrand's theory of the solubility of microsolutes in ordinary solvents, and of the Flory-Huggins theory to the solubility of steroids in polymers, has permitted the derivation of a predictive correlation between polymer permeability and steroid crystalline melting temperature, other correlating parameters being the entropy of fusion of the steroid and the (computed) solubility parameters of steroid and polymer. The correlation permits prediction of the permeability of any steroid in any polymer with reasonable accuracy.

A. S. MICHAELS, P. S. L. WONG, R. PRATHER, and R. M. GALE

ALZA Corporation
Palo Alto, California 94304